Meta-Analysis

Gray Matter Alterations in Medication Overuse Headache: A Voxel-Based Morphometry Meta-Analysis

Weiming Luo, MD[1,2], Yuke Teng, MD[1,2], Xingyao Chen, MD[1,2], Nuo Chen, MD[1,2], Xinyue Zhang, MD[1,2], Jun Zhou, MD[1,2], Siyuan Tao, MD[1,2], Peng Lai, MD[1,2], Qian Song, PhD[3], Xinyu Hao, PhD[4], Fanrong Liang, PhD[1,2], Zhaoxuan He, PhD[1,2], and Zhengjie Li, PhD[1-3]

From: [1]Acupuncture and Tuina School, Chengdu University of Traditional Chinese Medicine, Chengdu, Sichuan, China; [2]Key Laboratory of Acupuncture for Senile Disease (Chengdu University of TCM), Ministry of Education, Chengdu, Sichuan, China; [3]National Clinical Research Center for Chinese Medicine Acupuncture and Moxibustion, First Teaching Hospital of Tianjin University of Traditional Chinese Medicine, Tianjin, Tianjin, China; [4]Acupuncture and Tuina School, Chongqing College of Traditional Chinese Medicine, Chongqing, China

Address Correspondence:
Zhengjie Li, PhD
Acupuncture and Tuina School
Chengdu University of Traditional Chinese Medicine
Chengdu, Sichuan, China
E-mail: lzjbenjamin@163.com

Disclaimer: W. Luo, Y. Teng, X. Chen, and N. Chen contributed equally to this article. This study was supported by funds from the National Natural Science Foundation of China (82474657, 81973958), the Distinguished Young Scholars Project of Science and Technology Department of Sichuan Province (No. 2025NSFJQ0056), and the Open Project of National Clinical Research Center for Chinese Medicine Acupuncture and Moxibustion (NCRCOP20230011). The datasets analyzed in the current study are available from the corresponding authors upon reasonable request.

Conflict of interest: Each author certifies that he or she, or a member of his or her immediate family, has no commercial association (i.e., consultancies, stock ownership, equity interest, patent/licensing arrangements, etc.) that might pose a conflict of

Background: Medication overuse headache (MOH) is a secondary headache disorder associated with the chronic use of pain-relieving medications, leading to significant alterations in brain structure and function. Previous studies have shown inconsistent findings in gray matter (GM) changes in MOH patients, making it necessary to conduct a comprehensive meta-analysis to synthesize these results.

Objectives: The objective is to conduct a thorough review and meta-analysis of the consistency among voxel-based morphometry (VBM) neuroimaging studies that focus on MOH.

Study Design: Systematic review and meta-analysis.

Setting: This meta-analysis examined all VBM studies that involved the whole-brain alterations of MOH.

Methods: A comprehensive search of neuroimaging studies was conducted across 6 databases, including EMBASE, PubMed, Web of Science, Wan-Fang Database, China National Knowledge Infrastructure (CNKI), and Chongqing VIP, covering publications from the inception thereof to December 1, 2023. Two independent researchers performed quality assessment, data extraction, and study selection. Researchers performed a thorough examination of GM data in MOH, utilizing both activation likelihood estimation (ALE) and Anisotropic effect size-signed differential mapping (AES-SDM). Additionally, the research included clinical variables correlation analysis and subgroup analysis.

Results: A total of 8 studies were selected for analysis based on stringent screening criteria, resulting in the inclusion of 378 patients (comprising 191 patients with MOH and 187 healthy patients). The 2 different neuroimaging meta-analysis methods both revealed that MOH patients had increased amounts of GM in their cerebellar vermis, left red nuclei, and right medial dorsal nuclei. Additionally, MOH patients showed reductions in the GM of their left superior frontal gyri, left inferior frontal gyri, right precunei, and bilateral middle frontal gyri. Correlation analysis findings indicated that numerous cerebral areas were linked to clinical variables of MOH, including the duration of the condition, frequency of headaches, and patient age. MOH patients using different medications exhibited partially inconsistent GM alterations.

Limitations: The limited number of neuroimaging studies and the variability in methodologies across studies might have affected the robustness of the findings. Future research should address these gaps by exploring both structural and functional neuroimaging in diverse MOH subtypes.

Conclusion: Significant alterations in GM across various brain regions associated with pain processing, modulation, and reward have been observed in association with MOH. These observations contribute to a better understanding of the neural mechanisms underlying MOH and may potentially guide the development of specific therapeutic strategies. Additional studies are required to investigate whether GM changes can serve as potential biomarkers for diagnosing and treating MOH.

interest in connection with the submitted article.

Article received: 09-25-2024
Revised article received: 10-04-2024
Accepted for publication: 12-09-2024

Free full article: www.painphysicianjournal.com

Key words: Medication overuse headache, MRI, neuroimaging, gray matter, voxel-based morphometry, neuroimagers meta-analysis

Pain Physician 2025: 28:E115-E127

Medication-overuse headache (MOH) is a secondary headache disorder. The condition is defined as an experience of 15 or more headache days per month by patients with a history of primary headache (such as migraine and tension-type headache) who have regularly overused one or more medications intended for the acute or symptomatic treatment of headaches for over 3 months. MOH is the third most common type of headache, with a global prevalence of approximately 4.6% (1). The prevalence of MOH is higher in women than in men, and it is relatively higher in middle-aged (20-64 years) and older adults (≥ 65 years) (2). Over 50% of patients with chronic headaches are estimated to experience MOH (3). The damages caused by MOH are not limited to promoting headache permanence but also include the medications' potential to induce toxicity and addiction. For example, excessive use of ergotamine can lead to sensory nerve damage and central cognitive impairment, while nonsteroidal antiinflammatory drugs (NSAIDs) may cause gastrointestinal side effects, central sensory abnormalities, and numbness (4). Animal studies have shown that long-term exposure to triptans enhances the activity of the calcitonin gene-related peptide (CGRP) and nitric oxide (NO) systems, resulting in persistent abnormal pain (5). Some patients with MOH experience improved their headache symptoms after discontinuing overused medications. Only approximately one-third of MOH patients showed significant improvement in headache frequency after medication withdrawal during the 2-3–month follow-up period (6). The current treatments for MOH are far from satisfactory.

The pathophysiology of MOH is still poorly understood, which restricts the development of effective and safe treatments for the condition. In recent decades, advancements in neuroimaging techniques have provided valuable insights into the neural pathophysiology of MOH. Voxel-based morphometry (VBM) is an automated method for analyzing changes in brain density, particularly in voxel-wise comparison of alterations to the structure of gray matter (GM), such as local volume and density. In recent decades, an increasing number of VBM studies have demonstrated significant gray matter structural alterations in patients with MOH. For example, some studies indicate that compared to healthy controls, MOH patients exhibit decreased GM in their inferior frontal gyri, middle frontal gyri, rectal gyri, and precunei (7). Multiple studies have demonstrated structural abnormalities within key regions of the mesocortical-limbic circuits in patients with MOH, including reduced orbitofrontal cortex thickness and volume (8). However, several studies observed no alterations in cerebral structure between MOH patients and healthy controls (9). Due to differences in design, sample size, and other imaging variables among studies, the results are not yet consistent, making it challenging to obtain a clear and reliable understanding of GM changes in MOH. Consequently, it is crucial to synthesize current relevant neuroimaging research and perform a thorough neuroimaging systematic review and meta-analysis to enhance our understanding of the neuropathological and symptomatic aspects of MOH.

Coordinate-based meta-analysis of neuroimaging studies involves combining multiple independent studies that share a common hypothesis. This type of meta-analysis uses objective, automated statistical methods and significance thresholds to estimate consistently observable effects on brain regions (10). Nowadays, ALE (activation likelihood estimation) and AES-SDM (anisotropic effect-size seed-based d mapping) are the 2 most frequently used neuroimaging meta-analysis methods. In neuroimaging research, ALE considers the foci as spatial probability distributions centered on specified coordinates to evaluate consistency and identify consistent activation areas across studies (11). AES-SDM improves the reliability of voxel value estimation—instead of assigning probability values to voxels, an "effect size" metric is given, more emphasis is placed on the factors influencing the results, weighting is given to study precision, and the concept of an "anisotropic kernel" is introduced to

further optimize the reconstructed statistical images. The concept of "anisotropic kernel" was introduced to further optimize the reconstructed statistical images (12). The ALE method focuses on processing activation coordinates but may overlook other information, such as effect size, while the SDM method not only considers effect size but can also conduct subgroup analysis, meta-regression analysis, and more. To obtain convincing and comprehensive results, the integration of both ALE and AES-SDM methods in a meta-analysis represents a well-established approach.

Building on the aforementioned points, this study conducted a systematic summary and meta-analysis of the alterations in GM structure among MOH patients. The study aimed to do the following: integrate available morphometric results to determine GM changes in MOH patients compared to healthy controls (HCs), using both ALE and AES-SDM methods; examine the possible statistical associations between clinical factors and gray matter alterations in patients with MOH headache; and (iii) attempt to identify the potential GM changes of MOH patients across different subtypes (such as MOH with different primary headaches, with different medication uses, and so on).

Search Strategies

A comprehensive literature search was performed across 6 electronic databases up to December 30, 2023. The databases included PubMed, Web of Science, Excerpta Medica Database (EMBASE), China National Knowledge Infrastructure (CNKI), Wan-Fang Database, and Chongqing VIP, covering publications from their inception to the specified end date.

This study used the definition of a Cochrane collaboration meta-analysis and followed the Preferred Reporting Items for Systematic Reviews and Meta-Analyses (PRISMA) guidelines, but due to the methodological limitations of the study, registration was not applicable. The query criteria were as follows: (i) medication overuse OR medication overuse headache OR analgesic overuse; (ii) migraine OR headache; (iii) neuroimaging OR magnetic resonance OR imaging neuro-imaging; (iv) MRI OR structure OR cortical OR morphometry OR gray matter OR voxel-based; (v) (i) AND (ii) AND ((iii) OR (iv)).

The search methodology was adapted for compatibility with Chinese electronic databases. Furthermore, to identify potentially overlooked studies, the researchers examined review articles and scanned the bibliographies of the included papers.

Inclusion and Exclusion Criteria

Inclusion criteria for the articles were as follows: (i) being primary clinical studies; (ii) involving patients with a diagnosis of MOH according to the International Classification of Headache Disorders (ICHD); (iii) comparing VBM in MOH patients with HCs; (iv) reporting of neuroimaging acquisition parameters, such as standard stereotactic space (Talairach or MNI).

Exclusion criteria included: (i) being duplicate reports of the included studies; (ii) lacking control-group studies; (iii) including MOH patients with other organic diseases, such as disorders of hematopoiesis, the liver, the renal system, the endocrine system, or the immune system, or psychiatric disorders; (iv) having fewer than 7 individuals in either group.

Data Extraction

Literature selection was performed by 2 independent researchers (Weimin Luo and Nuo Chen). After the selection, a team of researchers extracted the study data into spreadsheets and reviewed it carefully for accuracy. The data deemed pertinent and therefore extracted encompassed (i) details about the publication (the title, the journal in which it was published, and the year it was released); (ii) demographic information (gender, sample size, age, and preferred hand); (iii) clinical variables (medication types, headache duration, attack frequency, and types of the primary headache); (iv) neuroimaging information (scanning technique, scanning area, and magnetic field strength); and (v) imaging data analysis (software used and its version, coordinate system, spatial coordinates, method of multiple comparison correction, MRI data statistical analysis method, and diameter of Gaussian kernel). If data were unavailable or confusing, the corresponding author of the study was contacted by phone or email. For research involving multiple timepoints or interventions, only the baseline measurements were included in the analysis.

Quality Assessment

The quality of each study was independently reviewed and evaluated by authors Peng Lai and Siyuan Tao. In the event of a rating disagreement, the study was discussed by a panel of authors to determine a consensus score. The quality assessment checklist can be seen in Supplementary Table S1.

Statistical Analysis To utilize both the AES-SDM and ALE methods, this study used, respectively, both SDM software version 5.15 (www.sdmproject.com/software)

and GingerALE version 3.0.2 (www.brainmap.org/ale/) to measure changes in the GM of MOH patients.

The AES-SDM method integrates the extracted peak coordinates and effect sizes by generating variance maps and effect sizes through the application of an anisotropic Gaussian kernel with a 20 mm half-width, giving greater effect sizes to voxels that exhibit stronger correlation with the peak (12). The study plots were calculated by voxel to obtain random effects means, accounting for the sample size, within-study variability, and between-study heterogeneity. Studies with larger participant pools had a more significant impact, since the mean plots were weighted according to the square root of each study's sample size. Following the calculation of the meta-analysis average, thresholds were implemented using default parameters (voxel threshold $P < 0.005$, peak height threshold $z > 1.00$, and cluster size threshold ≥ 10 voxels) (12). To investigate potential clinical implications, researchers conducted meta-regression analyses. These analyses aimed to examine the associations between cerebral alterations and various clinical factors, including headache frequency, patient age, and headache duration. To capture results at one of the slopes and extremes of the regression density, the threshold of probability was reduced to 0.005. Any findings in areas not identified during the main analysis were excluded. A random-effects model utilizing a Q-statistic (between studies) was employed to examine the statistics of individual clusters, aiming to verify the reproducibility and stability of the primary findings. This study also tried to analyze subgroups, such as MOH patients with different primary headaches (migraine and tension-type headache) and different types of medication overuse (NSAIDs, triptans, or combination medicines). Furthermore, to evaluate the replicability of the findings, a jackknife sensitivity analysis was performed. The jackknife method is a popular resampling method that provides estimates of the bias and a standard error of an estimate by recomputing the estimate from subsamples of the available sample.

The ALE evaluates whether significant spatial focus convergence exists across experiments, with the initial hypothesis being a random spatial relationship (13). Initially, ALE represents the focus as the peak of a 3D Gaussian distribution to account for the spatial uncertainty of each reported coordinate. This model takes into consideration the number of participants, with studies involving fewer individuals resulting in broader Gaussian distributions (14). For each experiment, the "model activation" map was generated by integrating the probability distributions, while accounting for the impact of multiple closely reported foci within a single study (15). The concatenated modeled activation maps were used to compute ALE scores for each voxel. Those scores were then evaluated against the null distribution and adjusted for multiple comparisons (13). Corrections for cluster-level family errors were applied with an uncorrected threshold of $P < 0.001$ and cluster-level thresholds of $P < 0.05$ (16). To visualize and compare the primary outcomes obtained from both methods, researchers utilized the software program Mango version 4.1 (www.mangoviewer.com/), a specialized tool for data visualization.

Results

Overview of the Included Studies

This search strategy yielded 2808 publications, from which 8 publications were ultimately included in this meta-analysis according to the inclusion and exclusion criteria (Fig. 1). The study ultimately included 378 individuals, consisting of 191 MOH patients with an average age of 40.67 years (SD = 10.75) and 187 HCs with an average age of 40.28 years (SD = 10.63). All the patients were right-handed. There was no statistically significant difference found between MOH patients and HCs in terms of age and gender ($P > 0.05$). Tables 1 and 2 provide a comprehensive overview of the demographic information, MRI data, and clinical parameters from the studies included in this analysis.

Primary Findings of Gray Matter Changes in Patients with MOH

AES-SDM Method

The AES-SDM results showed that the GM of the left thalamus, middle cerebellar peduncles, right anterior cerebellar lobe, and right fusiform gyrus were increased in patients with MOH. Meanwhile, the GM of the left superior-frontal gyrus, left medial superior-frontal gyrus, left infra-frontal gyrus orbital, left supra-frontal gyrus orbital, right precuneus, and right middle-frontal gyrus were decreased in MOH patients (Table 3).

ALE Method

The ALE results showed that in MOH patients, GM was increased in the left fusiform gyrus, left hippocampus, left red nucleus, left caudate head, left thalamus pulvinar, right parahippocampus, right anterior cingu-

late, bilateral cerebellum (declive, culmen, cerebellar tonsil), bilateral thalamus, bilateral cingulate gyrus, and bilateral substania nigra. Additionally, the GM of MOH patients' brains was reduced in the left inferior frontal gyrus, left precentral gyrus, left insula, left middle occipital gyrus, left lentiform nucleus, right medial frontal gyrus, right sub-gyral hippocampus, right claustrum, right culmen of vermis, and bilateral middle frontal gyrus, bilateral superior frontal gyrus, and bilateral precuneus (Table 4).

Both neuroimaging meta-analysis methods revealed that the GM was increased in the vermis of cerebellum, left red nucleus, and right medial dorsal nucleus in MOH patients. Furthermore, MOH patients showed reduced GM in their left superior frontal gyri, left inferior frontal gyri, right precunei, and bilateral middle frontal gyri (Fig. 2).

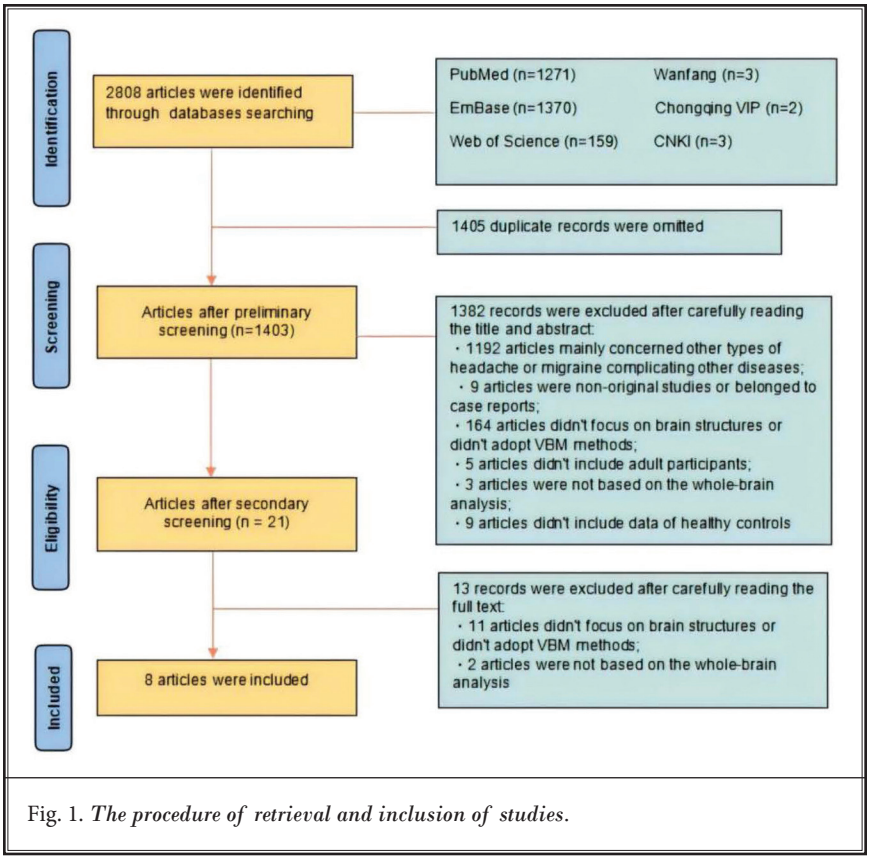

Fig. 1. *The procedure of retrieval and inclusion of studies.*

Meta-Regression Analysis

Meta-regression analysis was performed using only the AES-SDM method to investigate the potential correlations between clinical variables (duration of MOH disease, frequency of headache attacks, and age) and GM changes, since doing so was not possible with the ALE method (Suppl. Table S2).

The duration of illness in MOH patients was found to be positively correlated to increased GM in several brain regions, including the left median cingulate/paracingulate gyrus, left superior frontal gyrus, right thalamus, corpus callosum, bilateral cerebellum and bilateral striatum. In MOH patients, a positive correlation was observed between the frequency of headache episodes and GM volume in specific brain regions. Those areas included the left cerebellar hemisphere (lobule VIII) and vermis (lobules IV and V), the right middle cingulate and paracingulate gyri, and the right striatum. Conversely, MOH patients exhibited a negative correlation between headache attack frequency and GM in several brain regions, including the left hippocampus, right gyrus rectus, right superior longitudinal fasciculus, right lenticular nucleus putamen, and corpus callosum. Age was also found to be negatively associated with GM in the left superior frontal gyrus, corpus callosum, right gyrus rectus, right superior longitudinal fasciculus and bilateral hippocampus in MOH patients (Suppl. Table S2).

Subgroup Analysis

Traditional subgroup analyses were not possible for this manuscript, since the MOH patients in the included studies were not individually enrolled in either subtype of MOH headache (MOH patients with different primary headaches and who had overused different types of medication). However, to evaluate the potential effects of medication usage on MOH, the study analyzed the correlation between GM alterations and the usage of different medications in MOH patients (Suppl. Table S2).

The study was found that NSAID usage was positively associated with increased GM in the left median cingulate/cingulate gyrus, left cerebellar tonsils, right thalamus, right cerebellum (hemispheric lobule VIII),

Table 1. *Demographic and clinical characteristics of the patients in the included studies.*

Article	Sample Size		Mean Age (Years)		Female	Handedness	Mean Duration (Years)	Frequency of Attacks (per Month)	Aura	Primary Headaches	Overused Medication (Number of Patients)
	MOH	HC	MOH	HC							
Schmidt-wilcke et al. (42)	20	40	39.7	39.7	18	Right-handed	5.05	24.3	MA & MoA	19CM/1TTH	NSAIDs (13), triptans (1), combination analgesic (6)
Riederer et al. (48)	29	29	41.4 ± 12.7	41.7 ± 12.8	22	Right-handed	15.1 ± 11.0	22.7	MA & MoA	CM	NSAIDs (21), combination-analgesics (3), triptans (20), opioids (3)
Riederer et al. (49)	11	11	41.8 ± 9.1	44.3 ± 12.0	9	Right-handed	20.1 ± 12.2	25	MA & MoA	NA	NSAID (7), triptans (6), combination-analgesic (9)
Chanraud et al. (9)	17	17	46.3 ± 10.7	46.5 ± 10.5	13	Right-handed	29.4 ± 11.1	NA	NA	NA	Triptans (4), NSAIDs (2), opioid (2), combination-analgesic (1), unknown (8)
Lai et al. (7)	33	33	40.2 ± 10.0	39.7 ± 11.1	27	Right-handed	18.4 ± 10.4	23.2	MA & MoA	CM	NSAIDs (26), triptans (1), ergotamine (2), opioids (2), unknown (7)
Beckmann et al. (50)	27	27	37.9 ± 11.0	37.3 ± 7.9	21	Right-handed	7.2	22.9	MA & MoA	20CM/7TTH	NSAIDs (26), combination-analgesic (1)
Mehnert et al. (8)	18	18	36 ± 14	34 ± 9	13	Right-handed	20 ± 14	21	MA & MoA	CM	NSAIDs (12), triptans (5), combination-analgesic (1)
Chen et al. (51)	36	32	42.47± 9.34	41.34 ± 10.89	31	Right-handed	17.81 ± 5.81	NA	MA & MoA	CM	NA

MOH, medication overuse headache; HC, healthy control; NSAID, non-steroidal inflammatory drug; MA, migraine with aura; MoA, migraine without aura; CM, chronic migraine; TTH, tension type headache; NA, not available.

right cerebellar hemispheric lobule, corpus callosum, and bilateral striatum in MOH patients. Triptan usage was inversely correlated with GM changes in the left cerebellum (hemispheric lobule VIII), right gyrus rectus, right middle frontal gyrus, right inferior frontal gyrus, and corpus callosum. Additionally, combination medication usage showed positive correlations with GM changes in the left inferior semilunar lobule, left cerebellum (hemispheric lobule VI, VIII), left median cingulate/paracingulate gyrus, and right cerebellum (hemispheric lobule VI) and negatively correlations with GM changes in the left lentiform nucleus, right precuneus, right superior frontal gyrus (medial orbital), and right insula in MOH patients (Suppl. Table S2).

Heterogeneity Analysis and Sensitivity Analysis

Heterogeneity analysis showed significant heterogeneity among VBM studies with altered GM in brain regions, including the left superior medial frontal gyrus, left cingulum, right thalamus, bilateral cerebellum, bilateral hippocampus, and bilateral striatum $P < 0.05$ (Suppl. Table S3). The comprehensive jackknife sensitivity analysis conducted on the entire brain demonstrated high reproducibility across all regions (Suppl. Table S4).

Discussion

To our knowledge, this study is the first neuroimaging meta-analysis of MOH that uses the AES-SDM method with simultaneous verification of findings using the ALE method. This study confirms that MOH is significantly associated with GM alterations in various brain regions and networks, such as the cerebellar vermis, red nucleus, thalamus medial dorsal nucleus, inferior frontal gyrus, middle frontal gyrus, superior frontal gyrus, and precuneus. Correlation analyses demonstrated that GM alternations in MOH patients were also associated with clinical variables (such as MOH disease duration, headache frequency, and age) and could be influenced by the usage of medication.

Table 2. *MRI technique details of the included studies.*

Article	Imaging Technique	Scanner Magnetism	Statistical Analysis	Software	Correction for Multiple Comparison	Quality Score
Schmidt-wilcke et al. (2005)	MRI	1.5T	VBM	SPM99	$P < 0.05$, uncorrected	10
Riederer et al. (2012)	MRI	3.0T	VBM	SPM8	FDR $P < 0.05$	11
Riederer et al. (2013)	MRI	3.0T	VBM	VBM8/SPM8	FWE $P < 0.05$	10
Chanraud et al. (2014)	MRI	3.0T	VBM	SPM8	FDR $P < 0.05$	10.5
Lai et al. (2016)	MRI	1.5T	VBM	SPM8	FWE $P < 0.05$	11
Beckmann et al. (2018)	MRI	1.5T	VBM	FMRIB	TFCE $P < 0.05$	10.5
Mehnert et al. (2018)	MRI	3.0T	VBM	CAT12	FWE $P < 0.05$	10.5
Chen et al. (2018)	MRI	3.0T	VBM	SPM12	FDR $P < 0.05$	11

CAT, computational anatomy toolbox; FDR, false discovery rate; FWE, family-wise error; FMRIB, functional MRI of the brain; MRI, magnetic resonance imaging; SPM, statistical parametric mapping; TFCE, threshold-free cluster enhancement; T, tesla; VBM, voxel-based morphometry

Table 3. *Regional GM alterations between MOH patients and HCs using AES-SDM method.*

	Peak MNI Coordinate			SDM z-score[a]	*P*-value[b]	Number of Voxels[c]	Cluster Breakdown (Number of Voxels)
	X	Y	Z				
MOH > HS							
L thalamus	-2	-26	-6	1.747	~0	913	Left thalamus (497) Right thalamus (135) Right anterior thalamic projections (49)
R cerebellum	12	-44	-26	1.516	<0.001	712	Right cerebellum culmen (253) Middle cerebellar peduncles (106) Right cerebellum, crus I (69)
Middle cerebellar peduncles	-22	-38	-34	1.667	<0.001	316	Middle cerebellar peduncles (118) Left cerebellum, hemispheric lobule IV / V (52)
R fusiform gyrus	30	-48	-14	1.207	<0.001	23	Right fusiform gyrus (20)
MOH<HS							
L superior frontal gyrus, medial	0	56	0	-1.824	<0.001	1104	Right superior frontal gyrus, medial (228) Left superior frontal gyrus, medial (215) Left superior frontal gyrus, medial (113) Left anterior cingulate / paracingulate gyri (100)
R precuneus	8	-58	46	-2.109	~0	817	Right precuneus (198) Right precuneus (172) Corpus callosum (154) Right precuneus (113)
L inferior frontal gyrus, orbital part	-44	22	-8	-1.733	<0.001	387	Left inferior frontal gyrus, orbital part (169) Left inferior frontal gyrus, triangular part (80) Left inferior frontal gyrus, triangular part (52)
L superior frontal gyrus, orbital part	-12	40	-22	-1.508	<0.001	222	Left superior frontal gyrus, orbital part (75) Corpus callosum (47) Left gyrus rectus (22)
R middle frontal gyrus	40	50	12	-1.812	<0.001	209	Right middle frontal gyrus (81) Right middle frontal gyrus (75) Right superior frontal gyrus, dorsolateral (21)

AES-SDM, anisotropic effect size-signed differential mapping; BA, Brodmann area; GM, gray matter; MOH, medicine overuse headache; HC, healthy control; L, left; MNI, Montreal Neurological Institute; R, right.

[a] Peak height threshold: $z > 1$; [b] Voxel probability threshold: $P < 0.005$; [c] Cluster extent threshold: regions with < 20 voxels are not reported in the cluster breakdown

Table 4. *Regional GM alterations between MOH patients and HCs using GingerALE.*

	Peak MNI Coordinate			ALE Value (× 10–3)	Label (Nearest Gray Matter within 5mm)
	x	y	z		
MOH > HS					
Temporal Lobe	-39	-16	-30	6.61	L fusiform gyrus
	-27	-34	-3	7.99	L hippocampus
	28	-32	-5	7.44	R parahippocampus
Midbrain	-1	-22	-12	8.85	L red nucleus
	-11	-16	-12	7.49	L substania nigra
	10	-15	-12	7.49	R substania nigra
Striatum	-15	15	-7	7.48	L caudate head
Cerebellum	-27	-68	-12	8.54	L declive
	28	-64	-14	7.95	R declive
	-1	-33	-8	8.83	L culmen
	-18	-29	-30	8.52	L culmen
	1	-52	-24	6.61	R culmen
	18	-32	-30	8.82	R culmen
	-19	-51	-45	6.97	L cerebellar tonsil
	43	-63	-35	7.48	R cerebellar tonsil
Thalamus	-13	-24	2	6.61	L thalamus pulvinar
	-10	-24	2	9.12	L thalamus
	7	-22	4	6.61	R thalamus
Cingulate Gyrus	-7	-6	36	6.61	L cingulate gyrus
	1	-37	30	6.19	L cingulate gyrus
	7	19	-10	6.19	R anterior cingulate
MOH < HS					
Frontal Lobe	-45	32	-11	7.40	L inf frontal gyrus
	-16	38	-23	9.58	L mid frontal gyrus
	42	32	11	6.76	R mid frontal gyrus
	42	47	19	8.41	R mid frontal gyrus
	56	18	27	8.71	R mid frontal gyrus
	-3	60	15	8.14	L sup frontal gyrus
	27	60	1	7.99	R sup frontal gyrus
	3	38	27	7.44	R med frontal gyrus
	9	48	-23	7.22	R med frontal gyrus
	9	66	-5	7.99	R med frontal gyrus
	-46	18	1	7.44	L precentral gyrus
	-29	-9	65	7.88	L precentral gyrus
Temporal Lobe	32	-21	-9	6.75	R sub gyral hippocampus
	-43	-6	-6	8.54	L insula
Occipital Lobe	-16	-97	19	7.88	L mid occipital gyrus
Parietal Lobe	1	-52	50	7.49	L precuneus
	9	-63	46	8.56	R precuneus
Basal Ganglia	42	1	3	6.97	R claustrum
	-22	-15	-9	6.75	L lentiform nucleus
Cerebellum	7	-62	3	7.65	R culmen of vermis

Abbreviations: L, left; R, right; ALE, activation likelihood estimation; MNI, Montreal Neurological Institute; MOH, medicine overuse headache; HC, healthy control; GM, gray matter

The General Voxel-Based Morphometric Characteristic in MOH Patients

Through the AES-SDM and ALE methods, the meta-analysis revealed that patients with MOH showed overlapping GM alterations in the nociception, affection, and cognition aspects of their pain networks (thalamus medial dorsal nucleus, inferior frontal gyrus, middle frontal gyrus, superior frontal gyrus, precuneus, etc.), pain modulation systems (vermis of the cerebellum, red nucleus, inferior frontal gyrus, middle frontal gyrus, superior frontal gyrus, etc.), and reward systems (red nucleus, inferior frontal gyrus, middle frontal gyrus, superior frontal gyrus, etc.).

The thalamic medial dorsal nucleus serves as a crucial relay station for nociceptive messaging, receiving pain-related signals from the spinal cord, brain stem, and other thalamic nuclei before transmitting them to the prefrontal cortex (PFC) and other brain regions (17-19). Clinical studies have revealed that the thalamic medial dorsal nucleus exhibits altered activity in patients with chronic pain (20). The PFC is vital for regulating emotional and cognitive aspects of pain. The superior and inferior frontal gyri play a role in regulating emotions associated with pain and assist in managing the negative emotions that pain induces. Meanwhile, the middle frontal gyrus is responsible for the cognitive control of pain (20). The precuneus is a core hub in the default network (21). Studies have shown that chronic pain patients have

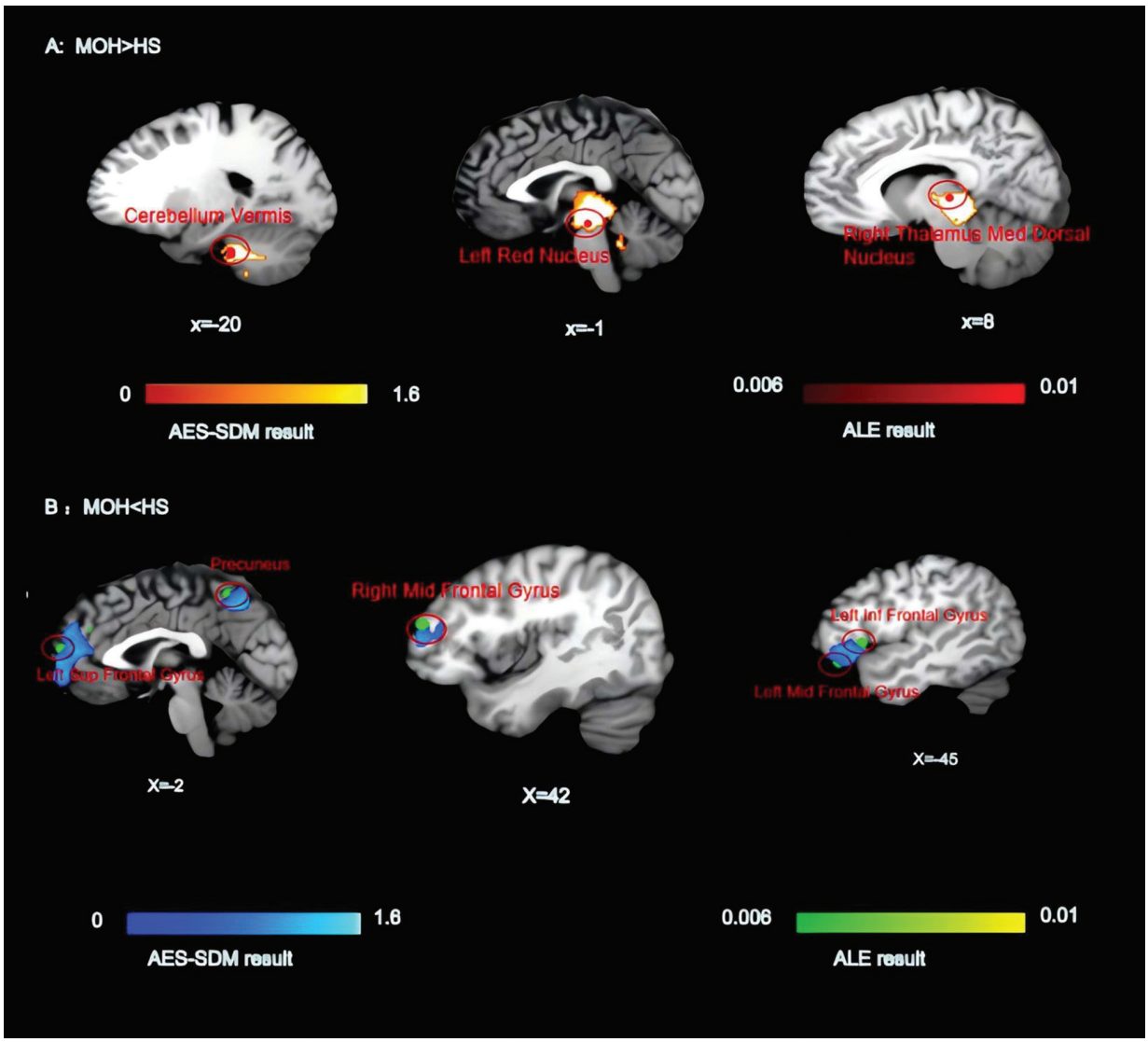

Fig. 2. *AES-SDM and ALE results investigating differences in GM between MOH patients and healthy controls.*
HS, healthy patients, AES-SDM, anisotropic effect size-signed differential mapping, ALE, activation likelihood estimation

altered precuneus functional connectivity within their default networks, potentially affecting these patients' persistent pain perception and emotional responses. The cerebellar vermis is also involved in the cognitive and emotional dimensions of pain-processing (22). The red nucleus, which is located at the central midbrain, is also involved in nociceptive modulation. Recent evidence suggests a causal relationship between the red nucleus and abnormal pain, which is mediated by recombinant pro-inflammatory cytokines in the red nucleus (23-26).

Approximately two-thirds of patients with MOH meet the diagnostic criteria for drug dependence (27). Abnormal GM alterations in the reward system are significant reflections of medication addiction in patients with MOH. The reward system, which mainly includes neural structures such as the ventral tegmental area (VTA), nucleus accumbens (NAc), PFC, and amygdala, is responsible for motivation, pleasure, and learning (28). However, the reward system can be "hijacked" by addictive substances, driving uncontrollable addictive behaviors. The present study found abnormal GM

alterations in MOH patients' reward systems, such as in the red nuclei and PFCs. The red nucleus is anatomically connected to other midbrain structures (such as the VTA) that are involved in reward-processing and dopamine release. Animal experiments have shown that glutamatergic neurons in the red nucleus project to the dopaminergic neurons in the VTA (29). The PFC is recognized as a crucial part of the reward system and is essential for working memory, decision-making, and impulse control (30). Specifically, the superior frontal gyrus is involved in anticipating and making decisions regarding rewarded behavior, the middle frontal gyrus assesses the social and emotional value of rewards, and the inferior frontal gyrus handles reward-related emotional changes. Recent brain imaging studies have found significant GM reductions in the frontal cortexes of patients with addictions. Addictive behaviors weaken self-control by altering PFC function and increasing impulsive behaviors, which may partially explain why patients with MOH readily repeat their medications (31).

The Voxel-Based Morphometry in MOH Patients is Related to Clinical Variables and Medication Usage

Clinical variables, such as disease duration, headache frequency, and age, were found to be significantly associated with changes to the GM of the MOH patients in this study.

The duration of MOH was positively correlated with GM alterations in specific brain regions, including the left cerebellar tonsil, left superior frontal gyrus, left middle cingulate/paracingulate gyrus, right thalamus, right cerebellum (hemispheric lobules VIII and IX), corpus callosum, and bilateral striatum. These regions are primarily involved in emotion-processing, cognitive regulation, and reward control. The cingulate cortex, particularly the anterior cingulate cortex, is a critical component of the pain matrix, and is involved in pain perception, emotion regulation, and cognitive control (32,33). Although the cerebellum has traditionally been regarded as a motor control center, it has also been implicated in pain perception (22). The striatum, including the caudate nucleus and putamen, is a key region in the dopamine-mediated reward system that receives signals from the orbitofrontal cortex, anterior cingulate cortex, and midbrain (34). The GM changes in these brain regions may result from prolonged recurrent headaches and medication overuse, potentially leading to heightened emotional responses to pain and abnormal activation of the reward system. The increasing duration of MOH not only indicates disease progression but also may be a major factor contributing to brain structural changes, underscoring the importance of early intervention in MOH treatment to prevent further brain damage.

The frequency of headache attacks in patients with MOH is closely linked to changes in the GM in several brain regions. Specifically, headache frequency was positively correlated with GM changes in the left cerebellum (hemispheric lobule VIII), right striatum, right middle cingulate/paracingulate gyri, and the cerebellar vermis (lobules IV/V). These regions are crucial for motor coordination, pain-processing, emotion regulation, and cognitive functioning (35-37). Conversely, headache frequency was negatively correlated with GM alternations in the right gyrus rectus, corpus callosum, left hippocampus, right superior longitudinal fasciculus III, and the right lenticular nucleus (putamen). These negative correlations suggest that frequent headaches may have detrimental effects on emotion regulation, cognitive function, and interhemispheric communication, possibly leading to the accumulation of negative emotions and increased medication use, thereby perpetuating a vicious cycle (38). Such observations indicate that the frequency of headache attacks not only affects pain perception and emotional responses in MOH patients but also may have profound negative impacts on brain structure and function, highlighting the need for targeted interventions that control attack frequency and mitigate structural brain damage.

As for age's influence on MOH patients' GM alterations, the notable reductions in the GM of the left superior frontal gyrus (orbital part), corpus callosum, right gyrus rectus, right superior longitudinal fasciculus III, and bilateral hippocampus may reflect age-related decline in cognitive function, emotion regulation, and information-processing abilities (39). These changes is not only a natural consequence of aging but also may be exacerbated by the long-term course of MOH and sustained medication use, further contributing to brain structural damage. Middle-aged and older patients with MOH may be particularly vulnerable to these changes, likely due to age-related brain atrophy and the cumulative effects of prolonged medication use.

The Voxel-Based Morphometry in MOH Patients is Different from That in Primary Headache Patients

MOH is a secondary headache caused by drug

overuse, whereas migraine and tension-type headaches (TTH) are the most common types of primary headaches (1). A recent meta-analysis of neuroimaging studies has revealed that individuals suffering from migraines exhibit GM changes in various cortical and subcortical brain regions. These alterations are primarily associated with sensory processing, emotional regulation, cognitive functions, and pain modulation mechanisms (40). Using the AES-SDM method, GM increases were observed in regions such as the bilateral temporal lobe (amygdala, parahippocampus, temporal poles, superior temporal gyri), the left hippocampus, and the frontal lobe (right superior frontal gyrus). GM decreases were found in the insula (left), cerebellum (bilateral, lobule IX), brain stem (right dorsal medulla), frontal lobe (right middle frontal gyrus), and parietal lobe (right inferior parietal gyrus). With the ALE method, GM changes were noted as increases in the parahippocampus (left) and decreases in the insula (left) in migraine patients. In TTH patients, significant GM alterations have been observed in multiple brain regions involved in pain processing (41). Studies have reported increased GM density in the bilateral anterior cingulate cortex (ACC) and anterior insula during headache episodes in patients with episodic TTH (42). Meanwhile, in the brains of patients with chronic TTH, a marked reduction in GM has been found in several regions, including the right cerebellum, brain stem tegmentum, bilateral anterior and posterior insula, bilateral orbitofrontal cortex, bilateral parahippocampal gyrus, right posterior temporal lobe, and anterior cingulate cortex (43).

Migraine and TTH sufferers may be more affected by the disease itself, whereas brain changes in MOH sufferers are influenced by both chronic primary headaches and medication addictions. These findings offer crucial insights into the complex neural pathology of MOH and provide potential therapeutic targets for MOH patients in the future. Discontinuation of analgesics and use of nonaddictive prophylactic medications are currently the main treatment choices in relieving the headaches of MOH patients (44). However, the efficacy of these treatments is not yet fully satisfactory. Fortunately, non-pharmacological therapies, including Tai Chi, acupuncture, and transcranial magnetic stimulation, have demonstrated promise in MOH management (45-47). The therapeutic targets of these combined interventions are likely to focus on one or more brain regions or networks that are aberrant in the cerebral tissues of patients with MOH.

Limitations

There are several limitations in this study: (1) Currently, the number of neuroimaging studies on MOH is limited. This study did not separately include MOH subtypes, which precluded the traditional subgroup analysis. Because MOH is classified as a secondary headache disorder, future research may benefit from conducting separate analyses on different categories of MOH patients. (2) This research focused solely on abnormal structural changes to the GM of patients with MOH. The study lacked neuroimaging meta-analyses that compared white matter tract mapping or functional alterations. Future clinical imaging investigations are necessary to gain a comprehensive understanding of both structural and functional changes in MOH patients' brains. (3) Studies may exhibit considerable variability. Differences in MRI equipment, image-processing techniques (including smoothing, registration, minor adjustments, data analysis approaches, and imaging techniques), characteristics of MOH patients (such as headache frequency, age, headache duration, and medication use), and HC inclusion criteria were observed across studies. The joint use of AES-SDM and ALE techniques might result in sufficient sensitivity and specificity for the findings. Although statistical methods were employed to account for and evaluate inter-study variations, caution should be exercised when interpreting this meta-analysis's results. As more research is published, this issue will need to be reevaluated. (4) The methodology employed in this systematic review relied on coordinate-based analysis rather than image-based or combined approaches, potentially introducing bias into the findings. To address this limitation, future research may benefit from the sharing of imaging data.

Conclusion

Patients with MOH show GM changes in several brain areas linked to nociception, affection and cognition aspects of the pain network, pain modulation system, and reward system. Additional studies are necessary to explore how these genetic modifications can be applied in diagnosing, tracking disease advancement, or creating potential treatments for patients with MOH.

References

1. Headache Classification Committee of the International Headache Society (IHS) The International Classification of Headache Disorders, 3rd edition. *Cephalalgia* 2018; 38:1-211.
2. Stovner LJ, Hagen K, Linde M, Steiner TJ. The global prevalence of headache: an update, with analysis of the influences of methodological factors on prevalence estimates. *J Headache Pain* 2022; 23:34.
3. Stark RJ, Ravishankar K, Siow HC, Lee KS, Pepperle R, Wang SJ. Chronic migraine and chronic daily headache in the Asia-Pacific region: A systematic review. *Cephalalgia* 2013; 33:266-283.
4. Cevoli S, Giannini G, Favoni V, et al. Treatment of withdrawal headache in patients with medication overuse headache: A pilot study. *J Headache Pain* 2017; 18:56.
5. De Felice M, Ossipov MH, Wang R, et al. Triptan-induced latent sensitization: A possible basis for medication overuse headache. *Ann Neurol* 2010; 67:325-337.
6. Scher AI, Rizzoli PB, Loder EW. Medication overuse headache: An entrenched idea in need of scrutiny. *Neurology* 2017; 89:1296-1304.
7. Lai TH, Chou KH, Fuh JL, et al. Gray matter changes related to medication overuse in patients with chronic migraine. *Cephalalgia* 2016; 36:1324-1333.
8. Mehnert J, Hebestreit J, May A. Cortical and subcortical alterations in medication overuse headache. *Front Neurol* 2018; 9:499.
9. Chanraud S, Di Scala G, Dilharreguy B, Schoenen J, Allard M, Radat F. Brain functional connectivity and morphology changes in medication-overuse headache: Clue for dependence-related processes? *Cephalalgia* 2014; 34:605-615.
10. Müller VI, Cieslik EC, Laird AR, et al. Ten simple rules for neuroimaging meta-analysis. *Neurosci Biobehav Rev* 2018; 84:151-161.
11. Turkeltaub PE, Eden GF, Jones KM, Zeffiro TA. Meta-analysis of the functional neuroanatomy of single-word reading: Method and validation. *Neuroimage* 2002; 16:765-780.
12. Radua J, Mataix-Cols D, Phillips ML, et al. A new meta-analytic method for neuroimaging studies that combines reported peak coordinates and statistical parametric maps. *Eur Psychiatry* 2012; 27:605-611.
13. Eickhoff SB, Bzdok D, Laird AR, Kurth F, Fox PT. Activation likelihood estimation meta-analysis revisited. *Neuroimage* 2012; 59:2349-2361.
14. Eickhoff SB, Laird AR, Grefkes C, Wang LE, Zilles K, Fox PT. Coordinate-based activation likelihood estimation meta-analysis of neuroimaging data: A random-effects approach based on empirical estimates of spatial uncertainty. *Hum Brain Mapp* 2009; 30:2907-2926.
15. Turkeltaub PE, Eickhoff SB, Laird AR, Fox M, Wiener M, Fox P. Minimizing within-experiment and within-group effects in Activation Likelihood Estimation meta-analyses. *Hum Brain Mapp* 2012; 33:1-13.
16. Eickhoff SB, Nichols TE, Laird AR, et al. Behavior, sensitivity, and power of activation likelihood estimation characterized by massive empirical simulation. *Neuroimage* 2016; 137:70-85.
17. Zhao DQ, Ai HB. Research progress of dorso-medial thalamic nucleus. *J U Jinan* 2016; 30:432-438.
18. Vogt BA, Sikes RW. The medial pain system, cingulate cortex, and parallel processing of nociceptive information. *Prog Brain Res* 2000; 122:223-235.
19. Apkarian AV, Baliki MN, Geha PY. Towards a theory of chronic pain. *Prog Neurobiol* 2009; 87:81-97.
20. Biggs EE, Timmers I, Meulders A, Vlaeyen JWS, Goebel R, Kaas AL. The neural correlates of pain-related fear: A meta-analysis comparing fear conditioning studies using painful and non-painful stimuli. *Neurosci Biobehav Rev* 2020; 119:52-65.
21. Cavanna AE, Trimble MR. The precuneus: A review of its functional anatomy and behavioural correlates. *Brain* 2006; 129:564-583.
22. Jie W, Pei-Xi C. Discharge response of cerebellar Purkinje cells to stimulation of C-fiber in cat saphenous nerve. *Brain Res* 1992; 581:269-272.
23. Basile GA, Quartu M, Bertino S, et al. Red nucleus structure and function: From anatomy to clinical neurosciences. *Brain Struct Funct* 2021; 226:69-91.
24. Cacciola A, Milardi D, Basile GA, et al. The cortico-rubral and cerebello-rubral pathways are topographically organized within the human red nucleus. *Sci Rep* 2019; 9:12117.
25. Steffens H, Rathelot JA, Padel Y. Effects of noxious skin heating on spontaneous cell activity in the magnocellular red nucleus of the cat. *Exp Brain Res* 2000; 131:215-224.
26. Ding CP, Guo YJ, Li HN, Wang JY, Zeng XY. Red nucleus interleukin-6 participates in the maintenance of neuropathic pain through JAK/STAT3 and ERK signaling pathways. *Exp Neurol* 2018; 300:212-221.
27. Radat F, Creac'h C, Guegan-Massardier E, et al. Behavioral dependence in patients with medication overuse headache: A cross-sectional study in consulting patients using the DSM-IV criteria. *Headache* 2008; 48:1026-1036.
28. Yang L, Zhang Y, Peng JT, Jiang YT, Cui MH. Research progress on the mechanism of dopamine reward system afferent regulation involved in depression. *J Neurosci Mental Health* 2024; 24:441-446.
29. Tzschentke TM, Schmidt WJ. Functional relationship among medial prefrontal cortex, nucleus accumbens, and ventral tegmental area in locomotion and reward. *Crit Rev Neurobiol* 2000; 14:131-142.
30. Tzschentke TM. The medial prefrontal cortex as a part of the brain reward system. *Amino Acids* 2000; 19:211-219.
31. Shi W, Li M, Zhang T, et al. GABA system in the prefrontal cortex involved in psychostimulant addiction. *Cereb Cortex* 2024; 34.
32. Peyron R, Laurent B, García-Larrea L. Functional imaging of brain responses to pain. A review and meta-analysis. *Neurophysiol Clin* 2000; 30:263-288.
33. Porro CA. Functional imaging and pain: Behavior, perception, and modulation. *Neuroscientist* 2003; 9:354-369.
34. Haber SN, Knutson B. The reward circuit: Linking primate anatomy and human imaging. *Neuropsychopharmacology* 2010; 35:4-26.
35. Xiao L, Bornmann C, Hatstatt-Burklé L, Scheiffele P. Regulation of striatal cells and goal-directed behavior by cerebellar outputs. *Nat Commun* 2018; 9:3133.
36. Jacobi H, Faber J, Timmann D, Klockgether T. Update cerebellum and cognition. *J Neurol* 2021; 268:3921-3925.
37. Vogt BA. Pain and emotion interactions in subregions of the cingulate gyrus. *Nat Rev Neurosci* 2005; 6:533-544.
38. Liu MG, Chen J. Roles of the hippocampal formation in pain information processing. *Neurosci Bull* 2009; 25:237-266.
39. Chen Y, Dang M, Zhang Z. Brain mechanisms underlying

neuropsychiatric symptoms in Alzheimer's disease: A systematic review of symptom-general and -specific lesion patterns. *Mol Neurodegener* 2021; 16:38.

40. Zhang X, Zhou J, Guo M, et al. A systematic review and meta-analysis of voxel-based morphometric studies of migraine. *J Neurol* 2023; 270:152-170.
41. Wang JL, Zhang SX, Sun XH. Research progress of multimodal MRI in tension-type headache. *Chin J MRI* 2022; 13:109-111+116.
42. Schmidt-Wilcke T, Leinisch E, Straube A, et al. Gray matter decrease in patients with chronic tension type headache. *Neurology* 2005; 65:1483-1486.
43. Chen B, He Y, Xia L, Guo LL, Zheng JL. Cortical plasticity between the pain and pain-free phases in patients with episodic tension-type headache. *J Headache Pain* 2016; 17:105.
44. He GD, Zhang ZJ. Treatment of overuse of medication for headache. *Chin J Pain Med* 2018; 24:763-767.
45. Teng Y, Luo W, Zhou J, et al. Clinical research on Tai Chi: A review of health benefits. *Acupuncture and Herbal Med* 2024.
46. Lu L, Chen C, Chen Y, et al. Effect of acupuncture for methadone reduction. *Ann Intern Med* 2024; 177:1039-1047.
47. Liu JL. Research on mechanisms of acupuncture analgesia - The most impressive field of acupuncture medicine. *World J Acupunct Moxibustion* 2023; 33:3-5.
48. Riederer F, Marti M, Luechinger R, et al. Grey matter changes associated with medication-overuse headache: Correlations with disease-related disability and anxiety. *World J Biol Psychiatry* 2012; 13:517-525.
49. Riederer F, Gantenbein AR, Marti M, et al. Decrease of gray matter volume in the midbrain is associated with treatment response in medicationoveruse headache: Possible influence of orbitofrontal cortex. *J Neurosci* 2013; 33:15343-15349.
50. Beckmann Y, Gökçe S, Zorlu N, et al. Longitudinal assessment of gray matter volumes and white matter integrity in patients with medication-overuse headache. *Neuroradiology J* 2018; 31:150-156.
51. Chen ZY, Chen XY, Liu MQ, et al. Volume gain of brainstem on medication-overuse headache using voxel-based morphometry. *Chin Med J* 2018; 131:2158-2163.

Table S1. *Quality Assessment Checklist (1 point per criterion for fully satisfied, 0.5 for partially satisfied, 0 for otherwise)*

Category 1: Subjects	Score (0/0.5/1)
1. Patients were evaluated prospectively, specific diagnostic criteria were applied, and demographic data were reported.	
2. Healthy subjects were evaluated prospectively, and psychiatric and medical illnesses were excluded.	
3. Important variables (such as age, gender, illness duration, onset time, medication status, comorbidity, and severity of illness) were checked, either by stratification or statistically.	
4. Sample size per group > 10.	
Category 2: Methods for image acquisition and analysis	
5. Magnet strength ≥1.5T.	
6. The whole-brain analysis was automatically calculated with no prior regional selection.	
7. Coordinates were reported in a standard space.	
8. The imaging technique processing was described clearly enough to be reproducible.	
9. Measurements were described clearly enough to be reproducible.	
Category 3: Results and conclusions	
10. Statistical parameters were provided.	
11. Conclusions were consistent with the results obtained and the limitations were discussed.	
	TOTAL /11

Table S2. *Meta-regression analysis of the correlation between GM alterations and clinical variables in MOH patients using the AES-SDM method*

	MNI coordinate			SDM z-score[a]	*P* value[b]	Number of voxels[c]	Cluster breakdown (number of voxels)
	X	Y	Z				
Duration							
L cerebellar tonsil	-16	-52	-46	3.775	<0.001	220	Left cerebellum, hemispheric lobule IX (67) Left cerebellum, hemispheric lobule VIII (42)
R thalamus	10	-22	4	4.805	<0.001	154	Right anterior thalamic projections (30) Right pons (21)
R cerebellum, hemispheric lobule VIII	34	-64	-46	3.331	0.001	67	Right cerebellum, hemispheric lobule VIIB (25)
L median cingulate / paracingulate gyri	-4	-6	36	3.517	<0.001	56	Left median network, cingulum (17)
Corpus callosum	26	-32	-4	3.612	<0.001	52	Right hippocampus (15)
L striatum	-12	14	-8	3.400	<0.001	55	Left lenticular nucleus, putamen (6)
R striatum	10	18	-10	3.376	<0.001	42	Corpus callosum (13)
R cerebellum, hemispheric lobule IX	12	-56	-44	3.133	0.001	35	(undefined) (14)
L superior frontal gyrus	2	40	28	2.859	0.001	29	Left anterior cingulate / paracingulate gyri (6) Right anterior cingulate / paracingulate gyri (6)
Frequency							
L cerebellum, hemispheric lobule VIII	-18	-72	-52	1.085	<0.001	236	Left cerebellum, hemispheric lobule IX (27) (undefined) (66)
R striatum	-4	14	-12	1.081	<0.001	112	Left olfactory cortex (12) Right olfactory cortex (12)
R median cingulate / paracingulate gyri	2	-48	36	1.078	<0.001	64	Left posterior cingulate gyrus (9) Right precuneus (6)
Cerebellum, vermic lobule IV / V	4	-60	-14	1.081	<0.001	46	Cerebellum, vermic lobule IV / V (12) Cerebellum, vermic lobule VI (5)
R gyrus rectus	8	50	-18	-2.810	<0.001	319	Right superior frontal gyrus, orbital part (67) Corpus callosum (52)
Corpus callosum	12	-54	52	-3.165	<0.001	284	Right precuneus (84) Right precuneus (55)
L hippocampus	-22	-12	-8	-2.511	<0.001	82	Left pons (19) (undefined) (20)
R superior longitudinal fasciculus III	40	30	14	-2.224	0.001	70	Right inferior frontal gyrus, triangular part (10)
R lenticular nucleus, putamen	34	-18	-4	-2.187	0.001	22	Right inferior network, inferior fronto-occipital fasciculus (6) Corpus callosum (5)
Age							
L superior frontal gyrus, orbital part	-12	38	-24	-2.265	<0.001	493	Corpus callosum (118) Left gyrus rectus (72)
R gyrus rectus	8	46	-20	-2.082	<0.001	308	Right superior frontal gyrus, orbital part (69) Corpus callosum (59)
Corpus callosum	14	-58	50	-2.234	0.001	277	Right precuneus (51) Right precuneus (24)
R superior longitudinal fasciculus III	42	34	16	-2.169	<0.001	250	Right inferior frontal gyrus, triangular part (68) Right middle frontal gyrus (67)
L hippocampus	-20	-14	-10	-1.904	<0.001	91	Left pons (18) (undefined) (22)
R hippocampus	30	-20	-10	-1.843	0.001	70	Corpus callosum (7) Right optic radiations (5)

Table S2 cont. *Meta-regression analysis of the correlation between GM alterations and clinical variables in MOH patients using the AES-SDM method*

	MNI coordinate			SDM z-score[a]	*P* value[b]	Number of voxels[c]	Cluster breakdown (number of voxels)
	X	Y	Z				
NSAIDs							
L cerebellar Tonsil	-16	-52	-46	3.904	<0.001	263	Left cerebellum, hemispheric lobule IX (84) Left cerebellum, hemispheric lobule VIII (62)
R thalamus	10	-22	4	4.901	<0.001	160	Right anterior thalamic projections (31) Right pons (21)
R cerebellum, hemispheric lobule VIII	34	-64	-46	3.403	0.001	70	Right cerebellum, hemispheric lobule VIIB (25) Right cerebellum, crus II (9)
L striatum	-12	14	-8	3.503	<0.001	59	Left lenticular nucleus, putamen (6) Left anterior thalamic projections (4)
L median cingulate / paracingulate gyri	-4	-6	36	3.585	<0.001	56	Left median network, cingulum (17) Left median cingulate / paracingulate gyri (9)
Corpus callosum	26	-32	-4	3.676	<0.001	53	Right hippocampus (15)
R striatum	10	18	-10	3.528	<0.001	54	Corpus callosum (16) Right gyrus rectus (6)
R cerebellum, hemispheric lobule IX	12	-56	-44	3.210	0.001	35	Right cerebellum, hemispheric lobule VIII (1) (undefined) (14)
Triptans							
R gyrus rectus	8	28	-18	-2.243	<0.001	318	Corpus callosum (69) Left gyrus rectus (40)
Corpus callosum	-16	28	-16	-1.862	0.001	322	Left superior frontal gyrus, orbital part (83) Left gyrus rectus (42)
L cerebellum, hemispheric lobule VIII	-22	-58	-58	-1.954	0.001	195	Left cerebellum, hemispheric lobule IX (5) (undefined) (36)
R middle frontal gyrus	48	42	12	-1.866	0.001	160	Right inferior frontal gyrus, triangular part (24) Right middle frontal gyrus (12)
Corpus callosum	14	-60	42	-1.788	0.001	43	Right precuneus (2) Right superior parietal gyrus (1)
R inferior frontal gyrus, triangular part	50	20	26	-1.703	0.001	20	Right inferior frontal gyrus, triangular part (5) Right inferior frontal gyrus, opercular part (4)
Combination Medication							
R cerebellum, hemispheric lobule VI	30	-62	-32	1.308	<0.001	167	Right cerebellum, hemispheric lobule VI (26) Right cerebellum, hemispheric lobule VIII (26)
Left Inf semi-Lunar lob	-8	-66	-46	1.308	<0.001	84	Left cerebellum, hemispheric lobule IX (20) Cerebellum, vermic lobule IX (15)
R cerebellum, posterior lobule	42	-48	-44	1.308	<0.001	35	Right cerebellum, hemispheric lobule VIII (11) Right cerebellum, hemispheric lobule VIIB (3)
L cerebellum, hemispheric lobule VI	-18	-70	-20	1.307	<0.001	28	Left lingual gyrus (5) Left inferior network, inferior longitudinal fasciculus (4)
L median cingulate / paracingulate gyri	-4	-28	40	1.308	<0.001	25	Right median cingulate / paracingulate gyri (8) Left median cingulate / paracingulate gyri (5)
L cerebellum anterior lobule	-4	-54	-28	1.308	<0.001	24	Cerebellum, vermic lobule IV / V (6) Left cerebellum, hemispheric lobule IV / V (3)
L cerebellum, hemispheric lobule VI	-30	-54	-18	1.308	<0.001	23	Left cerebellum, hemispheric lobule VI (7) Left fusiform gyrus (6)
L cerebellum, hemispheric lobule VIII	-26	-64	-44	1.308	<0.001	20	Left cerebellum, hemispheric lobule VIIB (1) (undefined) (5)
R precuneus	12	-58	60	-1.966	~0	924	Right precuneus (211)

Table S2 cont. *Meta-regression analysis of the correlation between GM alterations and clinical variables in MOH patients using the AES-SDM method*

	MNI coordinate			SDM z-score[a]	*P* value[b]	Number of voxels[c]	Cluster breakdown (number of voxels)
	X	Y	Z				
R superior frontal gyrus, medial orbital	6	58	-14	-1.965	~0	519	Right superior frontal gyrus, medial orbital (75) Right gyrus rectus (71)
R insula	34	-8	4	-1.688	0.001	287	Right lenticular nucleus, putamen (104) (undefined) (56)
L lentiform nucleus	-30	-8	-4	-1.766	0.001	281	Left lenticular nucleus, putamen (48) Left striatum (24)

a Peak height threshold: z > 1.
b Voxel probability threshold: $P < 0.005$.
c Cluster extent threshold: regions with < 20 voxels are not reported in the cluster breakdown.
Abbreviations: AES-SDM, anisotropic effect size-signed differential mapping; GM, gray matter; L, left; MNI, Montreal Neurological Institute; NSAIDs, nonsteroidal anti-inflammatory drugs; R, right; SDM, signed differential mapping.

Table S3. *Heterogeneity of altered GM regions between MOH patients and HS in VBM studies using the AES-SDM method.*

Brain regions	MNI coordinate			SDM z-score[a]	*P* value[b]	number of voxels[c]	Brain regions
	x	y	z				
Left cerebellum	-16	-52	-46	3.563	<0.001	219	Left cerebellum
Right thalamus	10	-22	4	4.597	<0.001	153	Right thalamus
Right hippocampus	26	-32	-4	3.404	<0.001	53	Right hippocampus
Left cingulum	-4	-6	36	3.298	<0.001	55	Left median network, cingulum
Left striatum	-12	14	-8	3.182	<0.001	54	Left striatum
Right striatum	10	18	-10	3.159	0.001	43	Right striatum
Right cerebellum, hemispheric lobule IX	12	-54	-44	2.906	0.001	35	Right cerebellum, hemispheric lobule IX
Left superior frontal gyrus, medial	2	40	28	2.625	0.001	27	Left superior frontal gyrus, medial
Left hippocampus	-26	-34	-4	2.692	0.001	18	Left hippocampus

a Peak height threshold: z > 1; b Voxel probability threshold: $p < 0.005$; c Cluster threshold: Regions with less than 10 voxels are not reported. Abbreviations: GM, gray matter; HS, healthy subjects; L, left; R, right; MNI, Montreal Neurological Institute; AES-SDM, anisotropic effect size-signed differential mapping; VBM, voxel-based morphometry

Table S4. *Sensitivity analysis of VBM meta-analysis using the AES-SDM method.*

VBM studies	Increased GM regions				Decreased GM regions				
	L THA	R CER	MCP	R FG	L SFG	R PRE	L ORBinf	L ORBsup	R MFG
Schmidt-Wilcke et al.2005	×	×	✓	✓	×	✓	✓	×	✓
Riederer et al.2012	×	×	✓	×	✓	✓	✓	✓	×
Riederer et al.2013	✓	✓	✓	✓	×	✓	✓	✓	✓
Chanraud et al.2014	✓	✓	✓	✓	✓	✓	✓	✓	✓
Lai et al.2016	✓	✓	✓	✓	✓	✓	×	✓	×
Beckmann et al.2018	×	×	✓	✓	✓	✓	×	×	✓
Mehnert et al.2018	✓	✓	✓	✓	×	×	✓	×	✓
Chen et al.2018	×	×	×	✓	✓	✓	×	×	✓

Abbreviations: VBM, voxel-based morphometry; AES-SDM, anisotropic effect size-signed differential mapping; L, left; R, right; GM, gray matter; THA, thalamus; CER, cerebellum; MCP, Middle cerebellar peduncles; FG, fusiform gyrus; SFG, superior frontal gyrus; PRE, precuneus; ORB inf, inferior frontal gyrus orbital part; ORB sup, superior frontal gyrus orbital part; MFG, middle frontal gyrus.